Published in final edited form as:
J Am Chem Soc. 2013 March 27; 135(12): 4620–4623. doi:10.1021/ja312610j.

Redox-Activated Manganese-Based MR Contrast Agent

Galen S. Loving[‡], **Shreya Mukherjee**[‡], and **Peter Caravan**[*]
A. A. Martinos Center for Biomedical Imaging, Massachusetts General Hospital, Harvard Medical School, 149 13th Street, Suite 2301, Charlestown, Massachusetts 02129, USA

Abstract

Here we report a simple Mn coordination complex with utility as a redox-sensitive MR probe. The HBET ligand stabilizes both the Mn^{2+} and Mn^{3+} oxidation states. In the presence of glutathione (GSH), low relaxivity Mn^{III}-HBET is converted to high relaxivity Mn^{II}-HBET with a 3-fold increase in relaxivity, and concomitant increase in MR signal. Alternately, hydrogen peroxide can convert Mn^{II}-HBET to Mn^{III}-HBET with a reduction in MR signal.

Both intracellular and extracellular redox environments are tightly regulated in healthy tissues and are closely correlated with the physiological state of the cell.[1,2] However, this regulation is often disrupted during periods of cellular stress, damage or cell death.[3] While the dynamics of local redox status play an important role in mediating various biological processes such as cell-cycle progression, immune response and wound-healing,[3,4] persistent dysregulation of the extracellular redox environment has been linked to a number of pathologies including chronic inflammation,[3] neoplastic growth,[4] and cancer cell aggressiveness.[1,5,6] Indeed, the role of redox in tumor biology continues to be an area of active research and is the focus of many redox-activated prodrugs that are currently in devolpment.[7,8] New imaging methods will certainly facilitate these endeavors while further advancing our basic understanding of redox dynamics in relation to disease.

There have been several redox-activated molecular imaging probes reported, each of which employs a unique mechanism of activation to address specific aspects of redox environment. Some of these probes target tissues that are hypoxic (low oxygen tension),[9-12] as sometimes occurs in tumors. Positron emission tomography (PET) probes ^{18}F-fluoromisonidazole (^{18}F-MISO) and ^{64}Cu-diacetyl-bis(N^4-methylthiosemicarbazone) (^{64}Cu-ATSM) have been used clinically to image tumor hypoxia.[10,12] Electron paramagnetic resonance (EPR) imaging and spectroscopy probes based on redox-sensitive nitroxides have proven effective at detecting the relative abundance of thiols as well as other reducing species.[13,14] Magnetic resonance (MR) probes have also been reported. Examples include Gd(III) complexes in which the ligands are capable of forming reversible disulfide linkages with cysteine side-chains of extracellular proteins thereby providing an indirect view of local redox conditions,[15,16] a Mn(II)-porphyrin which undergoes oxidation to a Mn(III) species with lower relaxivity under normoxic conditions,[9] and recently, a pair of Eu(III) complexes that can be activated in the presence of ß-NADH through reduction of the pendant arms of the ligands.[17]

[*]**Corresponding Author**caravan@nmr.mgh.harvard.edu.
[‡]These authors contributed equally.

Supporting Information. Full experimental details of complex synthesis and characterization, relaxivity, cyclic voltammetry, GSH reduction and H_2O_2 oxidation kinetics, and MR imaging are supplied as Supporting Information. This material is available free of charge via the Internet at http://pubs.acs.org.

No competing financial interests have been declared.

MR is an attractive modality to image redox dynamics as it allows the interrogation of intact, opaque organisms in three dimensions at cellular resolution (~10 μm) on high field systems and submillimeter resolution on clinical scanners. The deep tissue penetration and high resolution of MR make it possible to directly translate findings from cells to mice to humans.

One approach to a redox-sensitive MR probe is to employ a redox-active metal ion. Gd(III), used in the majority of MR probes has only one stable oxidation state in aqueous media. Manganese, however, can exist stably in a number of oxidations states depending on the ligand field. High spin Mn(II) complexes can also yield relaxivities that are comparable to the best Gd(III) complexes,[18,19] and there has been much recent work on Mn(II) complexes as MR probes.[20-23] Here we propose a new class of redox-activated MR probes based on the Mn(II)/Mn(III) redox couple.

There are several requirements for a useful redox-activated MR probe: 1) a redox half-cell potential that is accessible to biologically relevant reducing agents like glutathione (GSH); 2) a ligand that stabilizes both oxidation states such that reduction or oxidation does not result in decomposition; 3) strong signal change upon activation, and ideally signal increase in the presence of pathology, i.e. a turn-on probe; and 4) kinetics that are rapid with respect to the imaging timescale.

A key design feature of a redox-active probe is to identify a ligand that stabilizes both oxidation states. EDTA forms a very stable 7-coordinate Mn (II) complex with one coordinated water co-ligand, and the 2+ oxidation state is strongly favored, Figure 1.[24-26] By contrast, changing two carboxylato donors to phenolato donors as in HBED or EHPG strongly favors Mn(III) complexes[27,28] with coordination number 6 and no inner-sphere water, Figure 1.[29] We hypothesized that HBET (Figure 1) with a ligand structure that is intermediate between EDTA and HBED – containing only one phenolato donor – could potentially exhibit metastability toward either oxidation state. The preferred oxidation state of such a species would therefore be highly sensitive to changes in redox environment. To test this hypothesis, we prepared manganese complexes of HBED, HBET, and EDTA to examine how the number of phenolate groups contributes to the half-cell potentials of the Mn(III)/Mn(II) redox couple. Cyclic voltammetry of Mn^{II}-HBET in TRIS buffer (Figure 2) shows a reversible oxidation peak at 0.356 V (vs. NHE), indicating the potential for using this molecule as a redox probe. Anodic (i_a) and cathodic current (i_c) are linear with the square root of scan rate (ν) over the range of 50 – 600 mV/s (figure 2b), indicating this is a diffusion controlled process.[30] On the other hand, Mn^{II}-EDTA and Mn^{III}-HBED display irreversible oxidation and quasi-reversible reduction peaks with half-cell potentials (Mn^{III}/Mn^{II}) of 0.633 V and 0.016 V respectively.

HBET (hydroxybenzylethylenediamine triacetic acid) was synthesized from reductive amination of mono BOC-protected ethylene diamine with salicaldehyde, followed by alkylation with t-butyl bromoacetic acid, and then acid deprotection to give the free ligand in overall 45% yield. The reaction of one equivalent of ligand with $MnCl_2$ led to Mn^{II}-HBET in 84% isolated yield. The Mn^{III}-HBET complex was synthesized in 38% yield by aerial oxidation of $MnCl_2$ in the presence of one equivalent of the ligand under basic conditions, followed by RP-HPLC purification. The HBET ligand stabilizes both oxidation states to the extent that Mn^{II}-HBET and Mn^{III}-HBET can be easily separated and isolated in their pure forms using a standard RP-HPLC system. Mn^{II}-HBET showed slight oxidation to Mn^{III}-HBET and no decomposition when incubated in phosphate (5% oxidation) or carbonate (35% oxidation) buffer, but no oxidation in citrate buffer for 1 hr at 37 °C, pH 7.4 Mn^{III}-HBET was inert under the same conditions. However, we observed complete ligand-exchange for both complexes when challenged with EDTA.

The T_1 relaxivities of the Mn^{II}-HBET and Mn^{III}-HBET complexes were measured independently at 1.4 T in Tris buffer (pH 7.4, 37° C) and the values were 2.76 mM^{-1} s^{-1} and 1.05 mM^{-1} s^{-1}, respectively. This difference in relaxivity is large considering that the Mn^{III} state still has four unpaired electrons, and may be attributed to the presence of an inner-sphere water for Mn^{II}-HBET (CN7), while Mn^{III}-HBET may lack this coordinated water (CN6). In Figure 3, we show a T_1-weighted MR image at 4.7 T of glass inserts containing either pure water or equimolar Mn^{III}-HBET or Mn^{II}-HBET. The presence of the paramagnetic complex results in higher signal intensity compared to pure water. The higher relaxivity of Mn^{II}-HBET is apparent in its brighter image. T_1 measurements at 4.7 T revealed a 3.3-fold higher relaxivity for the reduced Mn^{II}-HBET form, Figure 3. The higher relaxivity of Mn^{II}-HBET at 4.7T vs 1.4T is likely due to the difference in temperature for these measurements. The slower tumbling rate at room temperature (4.7T) results in a higher relaxivity.

The Mn^{III}-HBET complex is easily reduced to the Mn^{II} state in the presence of low millimolar quantities of GSH such that the equilibrium lies strongly in favor of the reduced form. This conversion appears to proceed directly to the product without the accumulation of any long-lived reaction intermediates or the formation of byproducts. This is demonstrated by the time-course experiment shown in figure 4b where the emergence of the Mn^{II}-HBET complex occurs simultaneously with the consumption of Mn^{III}-HBET. The progress of this reaction can also be followed in real-time by relaxometry (figure 4a) using conditions relevant for clinical imaging (1.4 T, 37° C), or by UV absorbance. Since the relaxivity of the Mn(II) complex is greater than that of the Mn(III) complex, the longitudinal relaxation rate of water protons ($1/T_1$) will increase in proportion to the concentration of Mn^{II}-HBET in the reaction. Direct conversion of the Mn(III) complex to the Mn(II) complex is further evidenced by the observation that the rate of formation of the Mn^{II}-HBET species is effectively equivalent to the consumption rate of the oxidized form as measured by UV absorbance (figure 4a).

On the other hand, Mn^{II}-HBET could not be oxidized by GSSG, but it could be converted to Mn^{III}-HBET by H_2O_2 (Figure S10). We observed that the oxidation of 0.5 mM Mn^{II}-HBET with 1 mM H_2O_2 reaches equilibrium within 4 minutes at 70% conversion. This result opens the additional possibility of imaging the production of reactive oxygen species, albeit through a decrease of MR signal.

A series of kinetic experiments were conducted at 37 °C (pH 7.4) to determine the empirical rate law for the reduction of Mn^{III}-HBET by glutathione. Mn^{III}-HBET exhibits an absorbance band at 375 nm ($\varepsilon = 1.38\times10^3$ M^{-1} cm^{-1}) in water that is not present in the UV spectrum of the Mn^{II}-HBET complex. This feature allowed us to easily monitor the reduction of Mn^{III}-HBET over time. We measured initial reaction rates at a three different GSH concentrations (5 mM, 10 mM and 20 mM). For each GSH concentration, the reaction was performed at four different initial concentrations of Mn^{III}-HBET (0.3 mM, 0.4 mM, 0.5 mM and 0.6 mM). Based on these experiments, we determined that the reaction was first-order in both [GSH] and [Mn^{III}-HBET] with an overall second-order rate constant of $(3.8\pm0.3)\times10^{-1}$ M^{-1} s^{-1}. Concentrations of reduced glutathione within the cell are typically 1-10 mM.[31] In that range, the half-life of the Mn^{III}-HBET complex is roughly 3 to 30 minutes. By comparison, the half-life in blood plasma – where glutathione levels are approximately three orders of magnitude lower[31] – would be greater than one week.

In conclusion, the Mn^{III}/Mn^{II}-HBET redox couple satisfies a number of the key criteria required of a useful probe for redox imaging. The redox half-cell potential is accessible to biologically relevant reducing agents like GSH and H_2O_2; it displays good signal enhancement upon reduction to the MR-active state; and the activation kinetics are

sufficiently rapid with respect to the imaging timescale. The redox properties of this system are well behaved and the intercon-version between the two oxidation states occurs via a simple and reversible one-electron process.

While the Mn-HBET system represents a useful prototype for a redox sensitive probe, further work is necessary for in vivo studies. The complexes were unstable to the EDTA challenge and increased stability may be required. The redox kinetics and/or potential may also need tuning to address specific biological questions. However, we note that the HBET ligand may readily be modified, e.g. by using a more preorganized diamine to increase stability,[32] or with appropriate aryl substituents to tune the redox potential. The ligand could also be modified to incorporate a moiety that imparts specific biological targeting. Finally, in vivo studies will require the need to deconvolute differences in relaxivity from differences in concentration to the MR signal, however strategies exist that rely on control probes[33] or bimodal imaging.[34] These avenues are currently under investigation.

Supplementary Material

Refer to Web version on PubMed Central for supplementary material.

Acknowledgments

Dr. Anna Moore is gratefully acknowledged for providing access to a spectrophotometer. The National Cancer Institute and National Center for Research Resources are thanked for financial support (CA161221 and RR14075).

Funding Sources

This work was supported in part by awards CA161221 from the National Cancer Institute and P41RR14075 from the National Center for Research Resources.

REFERENCES

1. Moriarty-Craige SE, Jones DP. Annu. Rev. Nutr. 2004; 24:481. [PubMed: 15189129]
2. Schafer FQ, Buettner GR. Free Radic. Biol. Med. 2001; 30:1191. [PubMed: 11368918]
3. Rubartelli A, Lotze MT. Trends Immunol. 2007; 28:429. [PubMed: 17845865]
4. Sarsour EH, Kumar MG, Chaudhuri L, Kalen AL, Goswami PC. Antioxid. Redox Signal. 2009; 11:2985. [PubMed: 19505186]
5. Chaiswing L, Oberley TD. Antioxid. Redox Signal. 2010; 13:449. [PubMed: 20017602]
6. Jonas CR, Ziegler TR, Gu LH, Jones DP. Free Radic. Biol. Med. 2002; 33:1499. [PubMed: 12446207]
7. Brown JM, Wilson WR. Nat. Rev. Cancer. 2004; 4:437. [PubMed: 15170446]
8. Graf N, Lippard SJ. Adv. Drug Deliv. Rev. 2012; 64:993. [PubMed: 22289471]
9. Aime S, Botta M, Gianolio E, Terreno E. Angew. Chem. Int. Ed. Engl. 2000; 39:747. [PubMed: 10760856]
10. Eschmann S-M, Paulsen F, Reimold M, Dittmann H, Welz S, Reischl G, Machulla H-J, Bares R. J. Nucl. Med. 2005; 46:253. [PubMed: 15695784]
11. Iwaki S, Hanaoka K, Piao W, Komatsu T, Ueno T, Terai T, Nagano T. Bioorg. Med. Chem. Lett. 2012; 22:2798. [PubMed: 22424977]
12. Wood KA, Wong WL, Saunders MI. Nucl. Med. Biol. 2008; 35:393. [PubMed: 18482676]
13. Bobko AA, Eubank TD, Voorhees JL, Efimova OV, Kirilyuk IA, Petryakov S, Trofimiov DG, Marsh CB, Zweier JL, Grigor'ev IA, Samouilov A, Khramtsov VV. Magn. Reson. Med. 2012; 67:1827. [PubMed: 22113626]
14. Kuppusamy P, Li H, Ilangovan G, Cardounel AJ, Zweier JL, Yamada K, Krishna MC, Mitchell JB. Cancer Res. 2002; 62:307. [PubMed: 11782393]

15. Menchise V, Digilio G, Gianolio E, Cittadino E, Catanzaro V, Carrera C, Aime S. Mol. Pharm. 2011; 8:1750. [PubMed: 21780833]
16. Raghunand N, Jagadish B, Trouard TP, Galons JP, Gillies RJ, Mash EA. Magn. Reson. Med. 2006; 55:1272. [PubMed: 16700014]
17. Ratnakar SJ, Viswanathan S, Kovacs Z, Jindal AK, Green KN, Sherry AD. J. Am. Chem. Soc. 2012; 134:5798. [PubMed: 22420507]
18. Aime S, Anelli L, Botta M, Brocchetta M, Canton S, Fedeli F, Gianolio E, Terreno E. J. Biol. Inorg. Chem. 2002; 7:58. [PubMed: 11862541]
19. Troughton JS, Greenfield MT, Greenwood JM, Dumas S, Wiethoff AJ, Wang J, Spiller M, McMurry TJ, Caravan P. Inorg. Chem. 2004; 43:6313. [PubMed: 15446878]
20. Drahoš B, Lukeš I, Tóth É . Eur. J. Inorg. Chem. 2012; 2012:1975.
21. Lee T, Zhang XA, Dhar S, Faas H, Lippard SJ, Jasanoff A. Chem. Biol. 2010; 17:665. [PubMed: 20609416]
22. Rolla GA, Tei L, Fekete M, Arena F, Gianolio E, Botta M. Bioorg. Med. Chem. 2011; 19:1115. [PubMed: 20801660]
23. Szabo I, Crich SG, Alberti D, Kalman FK, Aime S. Chem. Commun. 2012; 48:2436.
24. Oakes J, Smith EG. J. Chem. Soc., Faraday Trans. 1981; 77:299.
25. Richards S, Pedersen B, Silverton JV, Hoard JL. Inorg. Chem. 1964; 3:27.
26. Zetter MS, Grant MW, Wood EJ, Dodgen HW, Hunt JP. Inorg. Chem. 1972; 11:2701.
27. Frost AE, Freedman HH, Westerback SJ, Martell AE. J. Am. Chem. Soc. 1958; 80:530.
28. Patch MG, Simolo KP, Carrano C. J. Inorg. Chem. 1983; 22:2630.
29. Bihari S, Smith PA, Parsons S, Sadler P. J. Inorg. Chim. Acta. 2002; 331:310.
30. Bard, AJ.; Faulkner, LR. Fundamentals and Applications. 2nd ed.. Wiley; New York: 2001. Electrochemical Methods..
31. Banerjee R. J. Biol. Chem. 2012; 287:4397. [PubMed: 22147695]
32. Kalman FK, Tircso G. Inorg. Chem. 2012; 51:10065. [PubMed: 22974437]
33. Raghunand N, Howison C, Sherry AD, Zhang S, Gillies R. J. Magn. Reson. Med. 2003; 49:249.
34. Frullano L, Catana C, Benner T, Sherry AD, Caravan P. Angew. Chem. Int. Ed. Engl. 2010; 49:2382. [PubMed: 20191650]

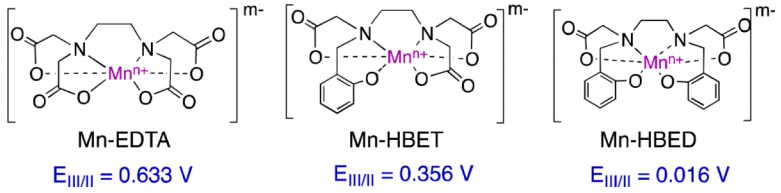

Figure 1.
Ligand structure strongly influences the redox potential of the Mn^{III}/Mn^{II} couple. Conversion of carboxylato to phenolato donors shifts the half-cell potential by 617 mV in favor of the higher oxidation state.

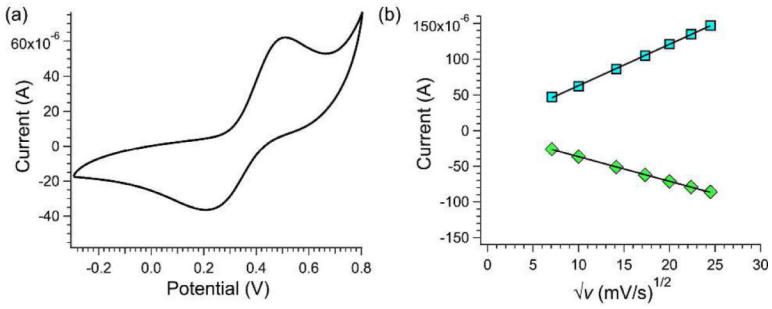

Figure 2.

(a) Cyclic voltammogram at 100 mV/s for 25 mM Mn^{II}-HBET in 25 mM pH 7.4 Tris buffer, 500 mM KNO_3, and $K_4Fe(CN)_6$ as an internal standard. Potentials reported vs NHE. (b) Cottrell plot of Mn^{2+}/Mn^{3+} couple - i_a (green) and i_c (blue) vs $\sqrt{\nu}$, where ν = scan rate.

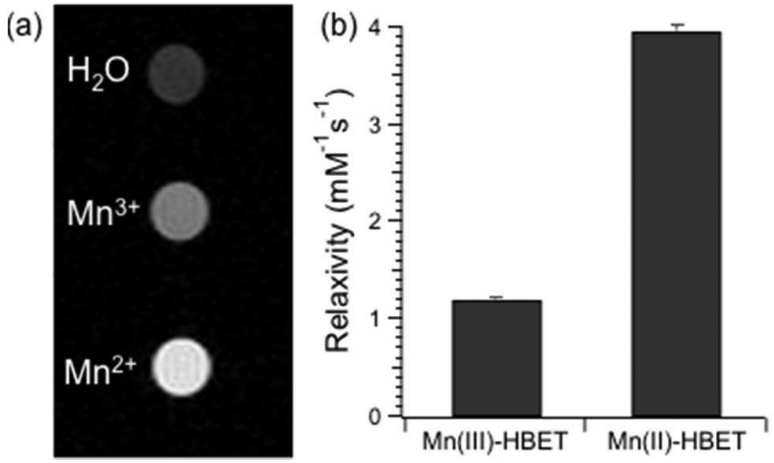

Figure 3.

Left: T_1-weighted MR image recorded at 4.7 T of tubes containing pure water, 0.5 mM Mn^{III}-HBET and 0.5 mM Mn^{II}-HBET in pH 7.4 TRIS buffer. Right: relaxivities measured at room temperature at 4.7 T.

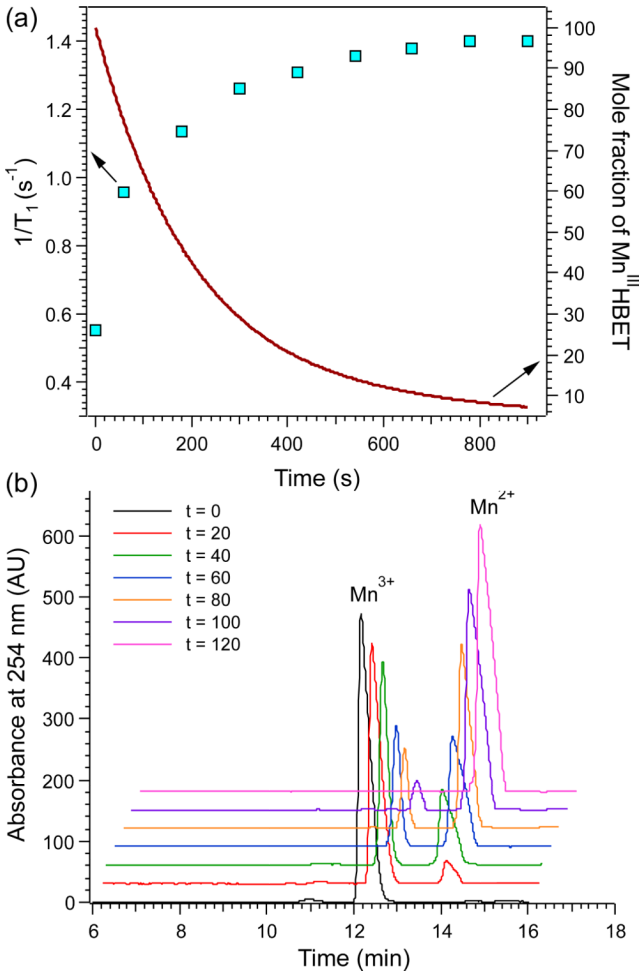

Figure 4.

(a) Reduction of 0.5 mM Mn^{III}-HBET to Mn^{II}-HBET by 10 mM GSH in TRIS buffer (pH 7.4, 37 °C) results in increased proton relaxation rate ($1/T_1$, left axis) and concomitant decrease in mole fraction of Mn^{III}-HBET (right axis) as determined by characteristic UV absorbance at 375 nm. (b) Reduction of 0.5 mM MnIII-HBET by 1 mM GSH at 26 °C monitored by LC-MS. No long-lived intermediate species were observed in the reduction process.